Ann. For. Res. 66(1): 1800-1817, 2023
ISSN: 18448135, 20652445

ANNALS OF FOREST RESEARCH
www.e-afr.org

AN OVERVIEW OF MICROWAVE DIELECTRIC SPECTROMETRY ON AQUEOUS MEDIUM

Jaya V Gade[1], Manzur Hassan[2], Neeta Gupta[3], Ajita Dixit[4], Pragya Awadhiya[5], Sarita Devi[6], Swati Mehra[7]*

[1]Department of Analytical Chemistry, SNDT Women's University, Mumbai 400049, Maharashtra India.

[2]Department of Zoology, Anundoram Borooah Academy Degree College, Pathsala, Bajali, Assam.

[3]Department of Chemistry, Govt. E. Raghavendra Rao P.G. Science College, Bilaspur, Chhattisgarh 495001 India.

[4]Department of Chemistry, Seth Phoolchand Agrawal College, Navapara, Rajim, Chhattisgarh 498831 India.

[5]Department of Applied Chemistry, Rungta College of Engineering and Technology, Raipur, Chhattisgarh 492001, India.

[6]Department of Chemistry, Dr. B.R. Ambedkar govt. P.G. college, Palwal, Haryana, 121102, India.

[7]*Department of Chemistry, IPS Academy, Institute of Engineering and Science, Indore, Madhya Pradesh 452012 India.

Abstract

The dielectric relaxation research on aqueous solutions is summarised to determine the relative strengths and limits of various solution models. Inorganic and organic electrolytes, as well as low-molecular-weight organic molecules, are among the solutes. It is demonstrated that even relatively simple solutions have a wide range of impacts. The hydration hypothesis appears to be validated due to the preferential orientation of water molecules in the Coulombic field of tiny ions and also in clathrate-like structures around big ions for solutions of such solutes. A hydration model appears to be appropriate for the solution of primarily hydrophobic compounds. Consequently, hydrophilic molecules are included in a hydrogen-bonded network. Many situations make it difficult to differentiate between the contributions of the solute and solvent molecules to the dielectric spectrum. Using such combinations, it is much more difficult to distinguish distinct water locations that have been influenced differently. In this review, we explored dielectric relaxation spectroscopy as a contemporary area of interest in aqueous solution. The dielectric characteristics of liquids at microwave frequencies are summarised, and the underlying molecular mechanisms and techniques are described. The peculiar behaviour of aquatic systems is given special consideration in this review.

Keywords: Dielectric spectroscopy, aqueous solution, spectroscopic techniques.

INTRODUCTION

Liquids are characterized by a short-range molecular order which rapidly varies in time. To monitor this order and its thermal fluctuations dielectric spectroscopy utilizes electrical charge distribution as naturally present molecular marks. Dielectric spectroscopy, which measures the complex permittivity of materials in a wide frequency range, is used in several areas, for example for the investigation of aqueous solutions with different molecular compositions. It is potentially very powerful as a marker and a permitted method for biomedical measurements1. In single cell and single particle analysis, the changes in dielectric properties are very small and must be measured with small amounts of liquid, which requires high sensitivity and broadband microwave measurements. Disintegrated salts significantly affect the dielectric properties of water: their ionic conduction definitely 2. Additionally, the static dielectric constant and the unwinding elements of the water atoms are essentially changed. The dielectric properties of electrolytes enormously affect an assortment of physical and synthetic properties and are additionally of significant importance2,3.

Lately, re-established interest emerged due to their significance for the absorption of electromagnetic radiation by organic matter. The entitled "Specific Absorption Rate" (SAR) for quantifying the absorption of electromagnetic radiation by living organisms is mainly determined by the conductivity of electrolytes, by the reflection coefficient. The physical quantity of the dielectric constant (έ) determines the radiation absorption by the body, and due to its influence on the wavelength, έ is also relevant for possible resonance effects in the organization. Hence, precise knowledge of the dielectric properties of electrolytes such as function of frequency, temperature and concentration of the ionic solution is extremely important4,5.

In this review we at first introduce the basic concepts lying behind the determining technique. Then the technique itself is reviewed, providing some of the solutions found useful by the authors in this review on aqueous systems.

BASIC PRINCIPLES OF DIELECTRIC SPECTROSCOPY

The dielectric spectroscopy (DS) strategy involves a unique position among the various present-day strategies utilized for physical and substance examinations of material. Since it empowers investigation

of dielectric unwinding measures in an incredibly wide scope of characteristic times. Even though the technique does not have the selectivity of nuclear magnetic resonance (NMR) or electron spin resonance (ESR), it offers significant and interesting data on the dynamic and underlying properties of substances. DS is particularly sensitive to intermolecular associations, and helpful cycles might be observed. It delivers a connection between the properties of the individual constituents of a complicated material and the description of its mass properties (figure 1).

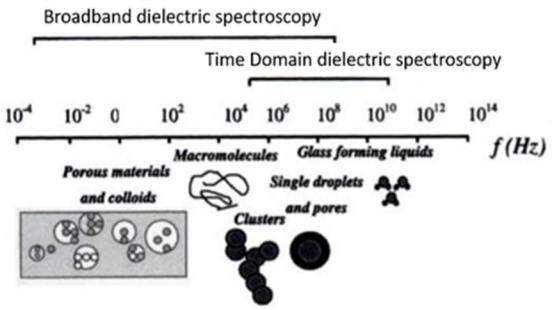

Figure 1: Electromagnetic wave scale of Dielectric Spectroscopy applicability for complex material 6.

Despite its long history of development, this method is not widely used because the wide frequency range (10-5-1012 Hz), superimposed by discrete methods in the frequency range, has required a lot of complex and expensive equipment. In addition, for various reasons, not all areas were available for the measurement equally. Investigations of samples with properties that change over time (e.g., unstable emulsions or biological systems) are difficult to carry out. Strong restriction due to the parasitic effect of the polarization of the electrode. All of the above-mentioned reasons meant that information about the dielectric properties of a substance could only be obtained in limited frequency ranges. This meant that only part of the dielectric spectrum was available to the researcher to determine the relaxation parameters.

The recent successful development of time domain dielectric spectroscopy (commonly referred to as time domain spectroscopy-TDS)5–7 and broadband dielectric spectroscopy (BDS)4,5 have radically changed outlooks towards DS and made it an effective tool made for the investigation of solids and liquids, on a macroscopic, microscopic and mesoscopic level. The basic approaches, the principles of experimental implementation, sample holders for various applications, data preparation and

presentation and various TDS methods that enable the entire spectrum of $\varepsilon^*(\omega)$ in the frequency range of 105 - 1010 Hz.

2.1 The Basic Principles of TDS Method

TDS is based on the time domain transmission line theory, which helps to investigate heterogeneities in coaxial lines based on the change in shape of a test signal. In the case of a heterogeneity in the line (e.g., the dielectric inserted in it) the signal is partially reflected from the air-dielectric interface and partially passes the dielectric measurements are along a coaxial transmission line carried out, with the sample being mounted in a sample cell terminating the line. The simplified block diagram of the common structure for most TDS methods (except transmission techniques) is shown in figure 2. The measuring cell and its position on the coaxial line. They lead to the different types of expressions for the values recorded during the measurement and the dielectric properties of the objects to be examined. A rapidly increasing voltage level V0(t) is applied to the line and recorded, together with the reflected voltage R(t), which is sent back from the sample and delayed by the duration of the initial time (figure 2). All instrument cables or artifacts are separated from the sample response due to the propagation delay, making them easy

to identify and control. The entire frequency spectrum is captured at once, eliminating drift and distortion between frequencies.

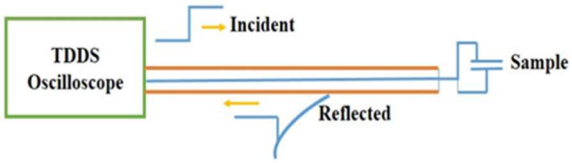

Figure 2 Basic TDS Set-up 6

The complex permittivity results as follows: For undispersed materials (frequency-independent permittivity) the reflected signal follows the exponential response RC of the line cell arrangement; with scattered materials, the signal follows a convolution of the line cell response with the frequency response of the sample. The actual sample response is found by writing the total voltage across the sample.

$$V(t) = V_0(t) + R(t) \quad (2.1)$$

And the overall current across the sample.

$$I(t) = \frac{1}{Z_0}[V_0(t) - R(t)] \quad (2.2)$$

Where the direction indicated by the sign change and Z0 is the characteristic line impedance. The aggregate current around a

conducting dielectric's is comprised of the displacement current ID(t), and the low-frequency current among the capacitor electrodes IR(t). Since the active resistance at zero frequency of the sample containing cell is (figure 3):

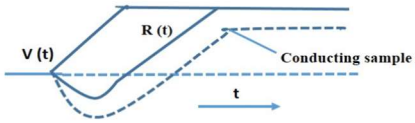

Figure 3 Characteristic shape of the signal recorded during a TDS experiment; V0(t): Incident pulse, R(t): Reflected signal 6

$$r = \lim_{t\to\infty}\frac{V(t)}{I(t)} = Z_0 \lim_{t\to\infty}\frac{V_0(t)+R(t)}{V_0(t)-R(t)} \quad (2.3)$$

The low-frequency current could be stated as:

$$I_R(t) = \frac{V(t)}{r} = \frac{V_0(t)+R(t)}{Z_0}\lim_{t\to\infty}\frac{V_0(t)-R(t)}{V_0(t)+R(t)} \quad (2.4)$$

Therefore relation (2.2) can be expressed as:

$$I_D\frac{1}{Z_0}\left\{[V_0(t) - R(t)] - [V_0(t) + R(t)]\lim_{t\to\infty}\frac{V_0(t)-R(t)}{V_0(t)+R(t)}\right\} \quad (2.5)$$

Relations (2.1) and (2.5) represent the fundamental equations that connect I(t) and V(t) to the signals documented throughout the experimentation. In addition, relation (2.5) indicates that TDS allows one to define the low-frequency conduction of the sample precisely in the time domain:

$$\sigma = \frac{\varepsilon_0}{Z_0 C_0}\lim_{t\to\infty}\frac{V_0(t)-R(t)}{V_0(t)+R(t)} \quad (2.6)$$

Where ε0 =8.85×10-12 F/m, and C0 is electric capacity of the coaxial sample cell terminated to the coaxial line. Applying I(t), V(t) or their intricate Laplace transforms i(ω) and v(ω) one can conclude the interactions that will illustrate the dielectric attributes of a sample being analyzed either in frequency or in time domain. The ultimate structure of these relations hangs on the geometric composition of the sample cell and its corresponding performance. The sample access for the sample cell ended to the coaxial line is then presented by,

$$Y(\omega) = \frac{i(\omega)}{v(\omega)} \quad (2.7)$$

And the sample permittivity could be represented as follows:

$$\varepsilon(\omega) = \frac{Y(\omega)}{i\omega C_0} \quad (2.8)$$

Where C0 is geometric capacitance of the blank sample cell. To reduce line objects and create a shared time reference, equation 2.7 is generally adjusted in differential form, to assess reflected indications from the sample and a standardized reference standard and therefore exclude V(t). If any takes into account the significant physical size of the sample and numerous expressions from the air-dielectric interfaces the relation (2.8) should be transcribed in the subsequent arrangement8 :

$$\varepsilon^*(\omega) = \frac{c}{i\omega(\gamma d)} Y(\omega) X \cot X \quad (2.9)$$

Where X= $(\omega d/c)\sqrt{\varepsilon^*(\omega)}$, d is the effective length of the inner conductor, c is the velocity of light, and γ is the ratio between the capacitance per unit length of the cell to that of the corresponding coaxial cable. Equation (2.9), in contrast to (2.8), is a transcendent one, and its precise resolution can be acquired only statistically9. The essential benefit of TDS techniques in contrast with frequency techniques is the capability to achieve the moderation attributes of a sample precisely in time domain. Resolving the integral equation one can calculate the outcomes in conditions of the dielectric response function Φ(t)6–8. It is then feasible to associate φ(t)=Φ(t)+ε_∞ with the macroscopic dipole correlation function Γ(t) in the context of linear response concept.

2.2 Experimental tools

2.2.1 Hardware

In order to meet the high demands of TDS measurements, such commercial devices must be significantly improved. The main problem lies in the fact that the detection of the incident V (t) and reflected R (t) signals is carried out by different measurements. In order to improve the signal-to-noise ratio, all recorded signals must be accumulated. The high degree of drift and instabilities during signal generation and detection on the sampler are often inherent in series reflectometry devices. The new generation of digital sampling oscilloscopes 7 and specially developed time domain measurement setups 10 offer a high-precision, comprehensive and automatic measurement system for TDS hardware support. They generally have a small fluctuation factor which is important to the rise time; low evenness of the incident pulse (two sampling channels are characterized by an 18 GHz bandwidth and 1.5 mV noise (RMS). Both channels are controlled by a common sample generator, which provides their chronological correspondence during operation. The time base is responsible for the most important TDMS measurement parameters. The block diagram of the TDS configuration described is shown in figure 4 10.

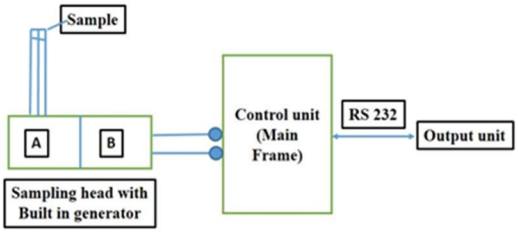

Figure 4 Circuit Diagram of the TDS Set-up 6

2.2.2 Software

The measurement, acquisition, storage, time referencing and data analysis processes in modern TDS systems are carried out automatically. The operating process is carried out in online mode and the results can be displayed in both the frequency and the time domain7,10–12. There are several functions of modern software that control the measurement and calibration process. During the calibration process the exact determination of the leading-edge position is carried out and the setting of the internal auto center in these positions is applied to all following measurements: The exact determination and setting of the horizontal and vertical positions of the calibration signals are also carried out. All parameters are saved in a configuration file. This enables a complete set of measurements to be made with the same parameters without additional calibration. It includes the options of signal correction, correction of electrode polarization and DC conductivity as well as various setting methods in both the time and frequency domain.

2.3 Electrode polarization corrections

Many dielectric materials are conductive. TDS investigation of conductive samples becomes very complex due to the polarization of the electrode and the need to correct for the effect of low frequency conductivity. Normally the DC conductivity value can be evaluated for a system with low conductivity. The biggest obstacle to TDS measurements of conductive systems is the dependent effect of electrode polarization. This accumulation of charge on the electrode surfaces leads to the formation of electrical double layers13–16. The associated capacitance and complex impedance due to this polarization is so great that correction is one of the main requirements in order to obtain meaningful measurements in conductive samples, especially in colloidal and biological aqueous systems14–17. The details of the electrode polarization microscopically depend on the electrode surface topography and surface as well as on the surface chemistry (reactive surface groups or atoms) and the interactions with the dielectric material. The ionization of the surface and the ion exchange processes in of the electrical
double layer depend crucially on the chemical nature of the sample to be examined as well as the chemical and physical nature of the electrodes used. Because these effects can be so different, no simple correction technique has become generally accepted. Several equivalent circuit diagrams have been proposed to describe the essential elements of a sample cell containing an electrolyte solution14,18 and the generally accepted approach. Two different approaches19 have been developed to correct this phenomenon in TDS measurements directly in the time domain. One of them can be used for weak electrolytes with low-frequency conductivity and thus a comparatively

low dependent effect of the electrode polarization19. The other approach, which is used in highly conductive systems, takes into account the fractal nature of the polarization of the electrodes.

2.4 External fields

The dielectric properties of a sample can be strongly influenced by its environment and measurements of the dielectric behavior such as function for example, temperature or pressure20 are carried out routinely. The TDS method also enables samples to be exposed to externally apply electric or magnetic fields.

2.4.1 Electric (High voltage measurements)

High electric fields were used to investigate the effect on w/o emulsions. In liquid crystal research, external electric fields are applied to ensure the desired orientation of the liquid crystals. The heads are very sensitive to high voltages and electrical currents, so the signal applied to a sample and consequently recorded by the TDS device must not exceed 0.2V. In order to achieve voltages between the electrodes that are high enough to cause changes in the sample and at the same time and over the same line the low-voltage pass pulse used in characterizing the sample is transmitted, special equipment must be used. In this way, a broadband coaxial polarization is inserted onto the transmission line. Which allows fast rise time pulses to pass with negligible waveform distortion while effectively preventing high voltage DC current from reaching the portion of the transmission line connected to the scan head. Modifications of the standard experimental setup required for this method. A DC voltage source is connected to the coaxial line as described above via a bias T-piece (Picsecond Pulse Labs, 5530A) so that strong voltages are generated between the electrodes of the electrode generates electric fields. With a 120μm spacer thickness and a potential difference of 60 V, the electric field applied to the sample is 5 kV/cm. This field strength is strong enough to cause a significant distortion of the shape of the water droplets in an emulsion, and in many cases the electric field induces the coalescence of the emulsion droplets. The T-piece and sampling head are additional protection of the sampling head against high voltage, only the through pulse is allowed to wander.

2.4.2 Magnetic fields

The orientation of a sample (on a molecular or aggregated level) through the action of a magnetic field can be achieved with a configuration21. The dielectric cell is of the type of an open coaxial sensor, and the electrical length was determined to be 0.027 mm. The magnetic field is generated with bar magnets, with the magnetic poles positioned on both sides of the dielectric cell used to measure the sedimentation profile of suspensions containing magnetic particles, in this case a magnetic field of approx. 0.4 T is generated by an electromagnet. The dielectric cell was also modified to increase the functionality of the experimental set-up.

DIELECTRIC PROPERTIES OF AQUEOUS SOLUTIONS

The static permittivity ε_(r)is required as input for models for Coulomb interactions between ions in a polar medium,22–26 such as the Debye-Hückel theory27 and the Born28 model of the free solvation energy. Hence, its derivatives are important to represent the chemical equilibrium and phase equilibrium in mixed electrolyte solutions,29 but unfortunately empirical models applied in

the context of thermodynamic models can introduce non-physical behavior. The presence of salts reduces the static dielectric constant of the mixture through kinetic polarization and the formation of layers of solvation around the ions, where the water binds through irritation, effectively eliminating its contribution to the dielectric relaxation of the solvent cation is said to coordinate 6-8 water molecules,30 while anions are supposed to coordinate a little less. The coordination number is typically estimated from hydrated molar volumes and ion diameters30,31. Despite the importance of static permittivity, there is no consensus on which terms to use when modeling electrolyte systems. Researchers have used ε_r from the pure or mixed solvent22,25,32,33 and some have considered the effect of ions through empirical models in which the calculated dielectric constant of the solvent is reduced by a factor 26. Others use non-primitive models in which the static permittivity is calculated implicitly within the equation of state itself from dipole-dipole, ion-dipole and ion-ion interactions34,35. To introduce methods for obtaining and analyzing data on the static permittivity of conductive liquids, there are several sources of systematic error that can occur when measuring experimental data or analyzing
data. These systematic errors have generally been ignored by electrolyte thermodynamics researchers, resulting in systematic errors in empirical models attempting to include the effect of static permittivity. Microscopic models to determine the effect of dielectric saturation and the way this information was used to develop continuous models through ion-solvent mixing and association rules. We present a review of the literature on the methods for calculating the static permittivity of aqueous salt solutions, including phenomenological models, and finally we present a new static permittivity model for mixtures of non-polar, polar and associated compounds, including electrolytes. This changes the Helmholt z-derivatives of the Debye-Hückel equation and compares the new model with a representative empirical model which are given below.

Modeling of Dielectric Saturation

The impact of dielectric immersion is brought about by the solid collaborations among dipoles and the electrical field encompassing the ions 27,30,36,37. This impact was demonstrated by Booth et al. 36, who derived a connection between the electrical field, the dipole snapshot of the dissolvable particles, and the spiral reliance of the dielectric immersion. The outcomes rely upon the model utilized for the nearby field, yet all arrangements might be addressed by the overall structure appeared in equation 3.1.

$$\left(\frac{\varepsilon(r)-n^2}{\varepsilon_r-n^2}\right)=\frac{3}{x}\left(\coth x-\frac{1}{x}\right) \quad (3.1)$$

In equation 3.1, $\varepsilon(r)$ gives the radial dependency of the inert permittivity as a distance from the center of an ion with charge q, $x=\left\{\frac{[\beta\mu_0(n^2+2)]}{[k_BT]}\right\}E(r)$, in which the deflective index, μ_0 is the vacuum permittivity, k_B is the Boltzmann constant, T is the temperature, E(r) is the electrical field from the ion with charge q given by $q[4\pi\varepsilon_r(r)\varepsilon_0 r^2]^{-1}$, and β is a constraint set to 1/2 when using the Onsager explanation of the local field,√73/6 when using the Kirkwood description, and 0.55 in the modified model [38]. Figure 3.1 represents the dielectric saturation outlines computed from equation 3.1 for the issue of ions with charges from 1 to 4 in water at 25°C assuming ε_∞= 2 and using β= 0.55.

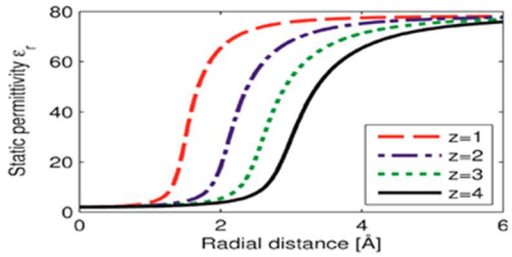

Figure 5 Dielectric Saturation Profile for Different ion Valences in Water using the Booth Model (equation 3.1)39.

Ion Solvation Model

The impact of dielectric screening might be addressed as a kind of particle solvation, where the atoms in the particle hydration shell do not add to the dipolar field as the dipoles are lined up with the electrical field of the ion40. The solvation models was first introduced by Hückel27, who decided the decrease in the dielectric steady utilizing the direct model appeared in equation 3.2, and showed how it improves the relationship of the action coefficient at high concentrations, c:

$$\varepsilon_r = \varepsilon_\omega - 2\delta c \qquad (3.2)$$

Ion Screening

An alternate methodology was introduced by Weiss and Schröer41, who considered the combination of equisized round particles and dipolar particle sets in the limited crude model. By comparing the energy from ion−dipole and dipole−ion cooperation energy, they acquired the articulation for the static permittivity as a component of ionic focus appeared in equation 3.3.

$$\frac{(\varepsilon_r-\varepsilon_\infty)[(2\varepsilon_r+\varepsilon_\infty)(1+k\sigma)+\varepsilon_r(k\sigma)^2]}{\varepsilon_r(1+k\sigma)} = \frac{\mu^2\rho_d}{\varepsilon_0 k_B T} \qquad (3.3)$$

Where ρ_ddensity of dipoles from the connotation of ions, κ is the inverse Debye length, and σ is the ion/dipole diameter. Weiss and Schröer41 applied their model to determine the static permittivity used for modeling of the phase performance of a pure ionic fluid, where equation 3.3 led to a considerable drop of the static permittivity due to shielding related to the Onsager model.

Field-Theory Approach

Using field-theoretical methods, Levy et al42. calculated the impact of particles on the static permittivity from a self-predictable arrangement of the Poisson−Boltzmann condition, utilizing equation 3.4 to portray the radial reliance of the static permittivity of a dissolvable with bulk permittivity ε_s:

$$\varepsilon_r(r) = \frac{\varepsilon_s}{3h^2(l_h/r)+1} \qquad (3.4)$$

In eq 3.4, l_h is a characteristic hydration length scale that depends on the dipole size and Bjerrum length and where the

function h(x) gives rise to a similar behavior as the Booth function. By resolving adjustment to the Gibbs free energy due to the hydration behavior, Levy et al. shows that the constant permittivity of water with salts can be computed using equation 3.5:

$$\varepsilon_r = \varepsilon_w + \frac{(\varepsilon_w-1)^2}{\varepsilon_w}\frac{4\pi}{3c_d a^3} - \frac{(\varepsilon_w-1)^2}{\varepsilon_w}\frac{k^2}{\pi c_d a}\left(1 - \frac{ka}{2\pi}\tan^{-1}\frac{2\pi}{ka}\right) \qquad (3.5)$$

In equation 3.5, cd is the dipole density and ε_w is the permittivity of water. Levy et al.42 suited the dipole moment and the ion size and achieved excellent connection with the constant permittivity of distinct salts in water.

Phenomenological Models

A collection of phenomenon-logical models is introduced in literature. Helgeson et al.43 represented a practical correlation amongst the dielectric constant of water ε_w and the dielectric constant of the solvent as shown in equation 3.6:

$$\varepsilon_r{}^{-1} - \varepsilon_w{}^{-1} = \sum_k b_k \Psi_k m_k \qquad (3.6)$$

In which m_k is the molality of the salt and b_k Ψ_k is a salt-specific constant suited to the intended decrease of dielectric constant. The authors noticed a linear correlation among the Gibbs energy of solvation and the decline of static permittivity. Wang and Anderko et al.29 modeled the impact of salts applying the empirical equation shown in equation 3.7.

$$\varepsilon_S \frac{\varepsilon_{s,0}}{1+\sum_i^{ions} A_i x_i ln\left(1+B_i\sqrt{I_X}\right)} \qquad (3.7)$$

In which ε_(s,0) is the static permittivity computed for pure solvent and ε_s is the constant permittivity of the medium involving salts. A_i and B_i are ion-specific parameters, and l_X is the ionic strength centered on mole fraction scale, as presented in equation 3.8:

$$l_X = \frac{1}{2}\sum_i^{ions} x_i \, z_i{}^2 \qquad (3.8)$$

Michelsen and Mollerup et al.44 presented another empirical model, while the empirical correlations according to equations 3.6 and 3.7 show a reasonably good agreement with the experimental data, which can be derived according to temperature, volume and configuration. In addition, these models do not take into account the significant contribution of kinetic depolarization, and this omission leads to a systematic error. This can lead to non-physical behavior of the static permittivity model and therefore influence the derivations of the electrostatic contributions to the Helmholtz energy 23. The static permittivity of aqueous salt solutions decreases due to the effect of dielectric saturation. However, the experimental data must be corrected for the dynamic contributions caused by kinetic depolarization in order to obtain the static permittivity for use in calculations of thermodynamic properties. Here it is shown that using an empirical model for static permittivity can introduce non-physical behavior into the derivatives of the electrostatic Helmholtz energy of the full Debye-Hückel equation. This model improves the physical description of the effect of solvents and solutes on static permittivity and electrostatic energy.

TYPES OF SPECTROSCOPY TECHNIQUES IN RESPECT TO AQUEOUS SOLUTIONS

The high dielectric constant between water and hydrocarbons provides a useful method of distinguishing between the producible layers of reservoir rock and the surrounding media. The dielectric response at high frequencies is related to the moisture content of the rock salt. The correlations between dielectric permittivity and specific surface area can be used to estimate the elastic and geo-mechanical properties of rocks. Knowledge of the dielectric dissipation factor and the relaxation frequency in shale is essential for the development of effective techniques for the

extraction of hydrocarbons from unconventional deposits. While the applicability of dielectric measurements is fascinating, the interpretation of the data is very difficult due to many factors that affect dielectric behavior. The dielectric constant is determined, for example, by the mineralogical composition of the solid fraction, the volume content and the composition of the saturation liquid, the microstructure of the rock and the geometric properties of its solid components and pores space, temperature and pressure. The frequency-dependent dielectric properties of artificial shale, which were made from mixtures of silt clay by mechanical compaction. The measurements of the dielectric properties are carried out in two orientations in order to investigate the dielectric anisotropy, since the samples acquire highly oriented microstructures during the densification process. The dielectric constant of a material is a measure of its frequency-dependent electrical polarization 45 in an applied external electrical field. In the presence of an electric field, electrons, ions and polar molecules contribute to frequency-dependent dielectric properties. In composite materials, the accumulation of charges at different conductivity boundaries and the formation of exchangeable cations can completely dominate the dielectric behavior. NaCl, for example, consists of liquid, solid and gaseous components and each of them is clearly defined by a certain chemical and / or mineral composition. A NaCl sample can reach many orders of magnitude in the high frequency range

(kilohertz to megahertz), which means that not only the components of a rock salt, but also its geometry, interaction, spatial arrangement and interfaces make a significant contribution to polarization46.

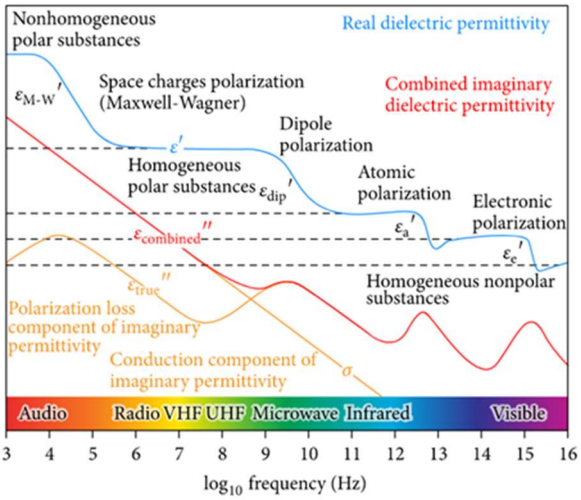

Figure 6 Schematics of dielectric polarization/conduction mechanisms, Josh47,48.

Dielectric measurements in the petrophysical and petroleum industries are mainly used to determine water content. Water molecules have a fixed electrical dipole moment and rotate rapidly to align with an external electrical field, while hydrocarbons have non-polar molecules and, as a result, have a much lower permittivity than water. Therefore, the estimation of the moisture content from the dielectric permittivity at high frequencies (> 1 GHz) is often used in borehole physics. In contrast, currently available commercial dielectric instruments operate with multiple point frequencies to facilitate the determination of water content and cation exchange capacity (CEC):

The dielectric response at frequencies below 50 MHz is more influenced by the surface effects described above. At lower frequencies, the clay content, the geometry and the spatial orientation of the mineral rock components as well as the salt content of the pore fluid also influence the measured dielectric constant 49. Some recent studies suggest alternative methods of oil production in unconventional reservoirs with dielectric heating50. This technology makes it possible to increase the profitability of exploration and it is largely based on the knowledge of the dielectric behavior in the frequency range of kilohertz-megahertz, where the penetration depth of the electric field is sufficient for field applications and the dielectric loss factor has maximum values 51. Various physical factors effect lead to a wide spread of the dielectric
relaxation peaks at frequencies below gigahertz. Determining the frequencies of the attenuation peaks as well as estimating the dielectric dispersion range for certain rock types would be helpful in adjusting the frequency of dielectric heating tools to ensure productive and energy efficient heating.

Another purpose of dielectric measurements is to estimate the CEC, a property that is directly attributed to the mineral composition and in particular the clay content. Josh 47 showed a strong correlation between the dielectric response at 30 MHz and CEC. This property is in turn linearly proportional to the specific surface area (SSA) of a rock salt, which determines the character and the amount of interparticle contacts (coordination number) under the given mineral composition and porosity of a rock. The dielectric constant has to be correlated with the static as well as with the dynamic elastic properties of a rock. Due to the complex composition of its mineral and liquid components, it is difficult to separate and study different factors that affect the dielectric properties of natural slates independently of one another. Studies on the frequency-dependent dielectric properties of rocks in relation to the component geometry (aspect ratios and orientation of mineral grains and pores), water saturation and organic content46,52,53. However, there is very little evidence from studies that take into account the clay content, microstructure and chemical composition of the pore fluid. The anisotropy of the dielectric properties of shale is critical to the interpretation of dielectric well logs, especially in deviated wells, and can affect production efficiency through dielectric heating in unconventional shale deposits 54. Again, there is little or no evidence, how the anisotropy of the dielectric properties of slate depends on the above parameters; the least known parameter regarding its influence on the dielectric response is the microstructure of the clay fraction in shale; different geological conditions can significantly influence the microstructure of the sediment and thus its properties 55. Dongand Wang 56 showed, that kaolinite sediments that are saturated with aqueous solutions with different pH values have significantly different dielectric spectra due to different microstructure formation mechanisms.

Dielectric spectroscopy, i.e., the measurement of the complex permittivity of materials in a wide frequency range, is used in several areas45, for the investigation of aqueous solutions with different molecular compositions. Dielectric measurements are potentially very powerful method for biomedical applications. In single cell and single particle analysis, the changes in dielectric properties are very small and must be measured with small amounts of liquid, which requires high sensitivity and broadband microwave measurements. Achieving high

sensitivity over a wide frequency range is challenging using traditional S-parameter-based techniques. Many different approaches to achieving high sensitivities have been explored, including electrode-based techniques47, cavity-based techniques, and techniques on transmission lines. Resonator-based techniques have achieved higher sensitivities. Techniques are greatly reduced when MUTs are applied at a loss, which degrades the effective quality factors. Techniques based on transmission lines generally have broadband characteristics. Further improvements are needed to improve the sensitivity for measurements at low concentration levels.

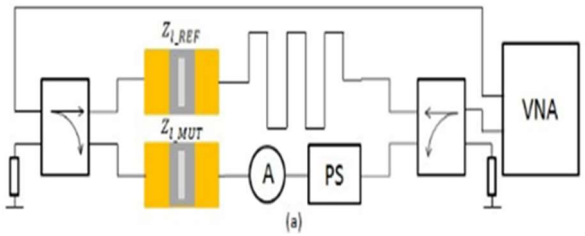

Figure 7 (a) A Representation of the microwave interferometer 48.

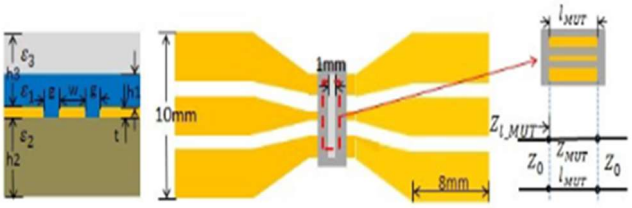

Figure 7 (b) The cross section and top view of the sensing structure with PDMS liquid well 48

In order to obtain deep interference zeros in our measurements, the design mainly focuses on building a better destructive interference between a reference branch and a MUT-loaded branch. Figure 7 shows the schematic of the microwave interferometer, which is based on two hybrids in quadrature broadband (QH, SigaTek, SQ16506, 4-18 GHz). The QH splits the microwave probe signal into a reference branch and a MUT loaded branch with phase difference between them to have destructive interference when they are combined again at the interferometer output. The tuning components are set on the MUT branch, a continuously tunable phase shifter and attenuator. The phase shifter (Arran 9428a, 0-18 GHz) is introduced to adjust the phase of a branch in order to obtain the phase difference between the two branches, tuning the depth of the interference zeros in a set of frequencies forms the operating frequencies to examine the MUT response. An attenuator (Narda 4799, 0-18 GHz) helps to compensate for the difference in attenuation caused by the QH, phase shifter,

CPW sensor structure, cables and connections. Different cable lengths are introduced into two branches because a greater difference between the cables in the two branches causes faster relative phase changes, thereby improving the sensitivity of the interferometer's transmission dispersion parameters. The attenuator is placed on the branch with the shorter cable length and the phase shifter can be configured on each branch as it has more than one phase shift. Due to the high sensitivity of the system, every cable or component movement influences the dispersion parameters, so a containment made of PMMA was developed to avoid unnecessary movements during operation and to make the structure more compact and flexible.

The configuration of the interferometer is described as simple production and connection to the system. It also simplifies modeling and data processing. The sensitivity also depends on the wave resistance of the detection structures; a higher sensitivity is achieved if the characteristic impedance of the central detection CPW with MUT within the microfluidic PDMS is closer to the measurement frequency. Hence, the CPW lines have been narrowed to achieve this.

CONCLUSION

The static permittivity of aqueous salt solutions decreases due to the effect of dielectric saturation. However, the experimental data must be corrected for the dynamic contributions caused by the kinetic depolarization in order to obtain the static permittivity for the calculation of the thermodynamic properties. A review of DS is presented as a powerful characterization technique for monitoring the dynamics of dipole moments in nanomaterials. The dielectric properties of materials generally play a major role in describing physical phenomena in various disciplines in natural, engineering and technical sciences. Fundamental studies of the dielectric behavior of nanomaterials provide a wealth of information about the various molecular movements and relaxation processes. Different polarization mechanisms prevail depending on the frequency of the applied field. The ability of TDS technique a non-invasive one to analyze in situ the properties of the intra-cellular structures is very important. This review also provides a brief introduction to DS and the basic concepts and methods of dielectric measurement of nanomaterials, types of dielectric spectroscopy techniques with respect to aqueous solvents are also discussed.

Reference

(1) Dai, L.; Zhao, X.; Guo, J.; Feng, S.; Fu, Y.; Kang, Y.; Guo, J. Microfluidics-Based Microwave Sensor. Sens. Actuators Phys. 2020, 309, 1–16. https://doi.org/10.1016/j.sna.2020.111910.

(2) Buchner, R.; Hefter, G. T.; May, P. M. Dielectric Relaxation of Aqueous NaCl Solutions. J. Phys. Chem. A 1999, 103 (1), 1–9. https://doi.org/10.1021/jp982977k.

(3) Chen, T.; Hefter, G.; Buchner, R. Dielectric Spectroscopy of Aqueous Solutions of KCl and CsCl. J. Phys. Chem. A 2003, 107 (20), 4025–4031. https://doi.org/10.1021/jp026429p.

(4) Peyman, A.; Gabriel, C.; Grant, E. H. Complex Permittivity of Sodium Chloride Solutions at Microwave Frequencies. Bioelectromagnetics 2007, 28 (4), 264–274. https://doi.org/10.1002/bem.20271.

(5) Stogryn, A. Equations for Calculating the Dielectric Constant of Saline Water (Correspondence). IEEE Trans. Microw. Theory Tech. 1971, 19, 733–736. https://doi.org/10.1109/TMTT.1971.1127617.

(6) Sjoblom, J.; Feldman, Y.; Skodvin, T. Dielectric Spectroscopy on Emulsion and Related Colloidal Systems—A Review; 2001; pp 109–168. https://doi.org/10.1201/9781420029581.ch6.

(7) Nozaki, R.; Bose, T. K. Broadband Complex Permittivity Measurements by Time-Domain Spectroscopy. IEEE Trans. Instrum. Meas. 1990, 39 (6), 945–951. https://doi.org/10.1109/19.65803.

(8) Feldman, Yu. D.; Zuev, Yu. F.; Polygalov, E. A.; Fedotov, V. D. Time Domain Dielectric Spectroscopy. A New Effective Tool for Physical Chemistry Investigation. Colloid Polym. Sci. 1992, 270 (8), 768–780. https://doi.org/10.1007/BF00776148.
(9) Folgero, K.; Friiso, T.; Hilland, J.; Tjomsland, T. A Broad-Band and High-Sensitivity Dielectric Spectroscopy Measurement System for Quality Determination of Low-Permittivity Fluids. Meas. Sci. Technol. 1995, 6 (7), 995–1008. https://doi.org/10.1088/0957-0233/6/7/022.
(10) Feldman, Y.; Andrianov, A.; Polygalov, E.; Ermolina, I.; Romanychev, G.; Zuev, Y.; Milgotin, B. Time Domain Dielectric Spectroscopy: An Advanced Measuring System. Rev. Sci. Instrum. 1996, 67 (9), 3208–3216. https://doi.org/10.1063/1.1147444.
(11) Miura, N.; Shinyashiki, N.; Yagihara, S.; Shiotsubo, M. Microwave Dielectric Study of Water Structure in the Hydration Process of Cement Paste. J. Am. Ceram. Soc. 1998, 81 (1), 213–216. https://doi.org/10.1111/j.1151-2916.1998.tb02317.x.
(12) Hager, N. E. Broadband Time-domain-reflectometry Dielectric Spectroscopy Using Variable-time-scale Sampling. Rev. Sci. Instrum. 1994, 65 (4), 887–891. https://doi.org/10.1063/1.1144917.
(13) Grant, E. H.; Sheppard, R. J.; South, G. P. Dielectric Behaviour of Biological Molecules in Solution; Monographs on physical biochemistry; Clarendon Press: Oxford, 1978.
(14) Lyklema, J. Fundamentals of Interface and Colloid Science. Volume 2: Solid-Liquid Interfaces. With Special Contributions by A. de Keizer, B.H. Bijsterbosch, G.J. Fleer and M.A. Cohen Stuart.; Academic Press: London, 1995; p .
(15) Bockris, J. O.; Reddy, A. K. N.; Gamboa-Aldeco, M. E. Modern Electrochemistry 2A: Fundamentals of Electrodics, 2nd ed.; Springer US, 2000. https://doi.org/10.1007/b113922.
(16) Schwan, H. P. Linear and Nonlinear Electrode Polarization and Biological Materials. Ann. Biomed. Eng. 1992, 20 (3), 269–288. https://doi.org/10.1007/BF02368531.
(17) Davey, C. L.; Markx, G. H.; Kell, D. B. Substitution and Spreadsheet Methods for Analysing Dielectric Spectra of Biological Systems. Eur. Biophys. J. 1990, 18 (5), 255–265. https://doi.org/10.1007/BF00188038.
(18) Niklasson, G. A.; Nettelblad, B. DIELECTRIC PROPERTIES OF WATER-CONTAINING POROUS MATERIALS: LOW FREQUENCY RESPONSE OF SANDSTONES. 9.
(19) Polevaya, Y.; Ermolina, I.; Schlesinger, M.; Ginzburg, B. Z.; Feldman, Y. Time Domain Dielectric Spectroscopy Study of Human Cells. II. Normal and Malignant White Blood Cells. Biochim. Biophys. Acta 1999, 1419 (2), 257–271. https://doi.org/10.1016/s0005-2736(99)00072-3.
(20) Böttcher, C. J. F.; Belle, O. C. van; Bordewijk, P.; Rip, A. Theory of Electric Polarization; Elsevier Scientific Pub. Co.: Amsterdam; New York, 1973.
(21) COLLOIDS AND SURFACES A PHYSICOCHEMICAL AND ENGINEERING ASPECTS: Ingenta Connect Table Of Contents https://www.ingentaconnect.com/content/el/09277757/1998/00000143/00000002 (accessed 2021 -06 -05).

(22) Y, L.; K, T.; Jc, de H. Multicomponent equations of state for electrolytes. AIChE J. 2007, 53 (4), 989–1005.
(23) Maribo-Mogensen, B.; Kontogeorgis, G. M.; Thomsen, K. Comparison of the Debye–Hückel and the Mean Spherical Approximation Theories for Electrolyte Solutions. Ind. Eng. Chem. Res. 2012, 51 (14), 5353–5363. https://doi.org/10.1021/ie2029943.
(24) Raatschen, W.; Harvey, A. H.; Prausnitz, J. M. Equation of State for Solutions of Electrolytes in Mixed Solvents. Fluid Phase Equilibria 1987, 38 (1), 19–38. https://doi.org/10.1016/0378-3812(87)90002-1.
(25) Wu, J.; Prausnitz, J. M. Phase Equilibria for Systems Containing Hydrocarbons, Water, and Salt: An Extended Peng−Robinson Equation of State. Ind. Eng. Chem. Res. 1998, 37 (5), 1634–1643. https://doi.org/10.1021/ie9706370.
(26) Simonin, J.-P.; Bernard, O.; Blum, L. Ionic Solutions in the Binding Mean Spherical Approximation: Thermodynamic Properties of Mixtures of Associating Electrolytes. J. Phys. Chem. B 1999, 103 (4), 699–704. https://doi.org/10.1021/jp9833000.
(27) 8 The Debye-Hückel theory and its importance in modeling electrolyte solutions - Fluid Phase Equilibria 2018.pdf | Chemical Equilibrium | Solubility https://www.scribd.com/document/416091250/8-The-Debye-Huckel-theory-and-its-importance-in-modeling-electrolyte-solutions-Fluid-Phase-Equilibria-2018-pdf (accessed 2021 -06 -05).
(28) Born, M. Volumen Und Hydratationswärme Der Ionen. Z. Phys. 1920, 1, 45–48. https://doi.org/10.1007/BF01881023.
(29) Wang, P.; Anderko, A. Computation of Dielectric Constants of Solvent Mixtures and Electrolyte Solutions. Fluid Phase Equilibria 2001, 186 (1–2), 103–122. https://doi.org/10.1016/S0378-3812(01)00507-6.
(30) Haggis, G. H.; Hasted, J. B.; Buchanan, T. J. The Dielectric Properties of Water in Solutions. J. Chem. Phys. 1952, 20 (9), 1452–1465. https://doi.org/10.1063/1.1700780.
(31) Marcus, Y. Electrostriction, Ion Solvation, and Solvent Release on Ion Pairing. J. Phys. Chem. B 2005, 109 (39), 18541–18549. https://doi.org/10.1021/jp051505k.
(32) Harvey, A. H.; Prausnitz, J. M. Thermodynamics of High-Pressure Aqueous Systems Containing Gases and Salts. AIChE J. 1989, 35 (4), 635–644. https://doi.org/10.1002/aic.690350413.
(33) Jin, G.; Donohue, M. D. An Equation of State for Electrolyte Solutions. 1. Aqueous Systems Containing Strong Electrolytes. Ind. Eng. Chem. Res. 1988, 27 (6), 1073–1084. https://doi.org/10.1021/ie00078a029.
(34) Liu, Z.; Wang, W.; Li, Y.-G. An Equation of State for Electrolyte Solutions by a Combination of Low-Density Expansion of Non-Primitive Mean Spherical Approximation and Statistical Associating Fluid Theory. 2005. https://doi.org/10.1016/J.FLUID.2004.11.007.
(35) Zhao, H.; dos Ramos, M. C.; McCabe, C. Development of an Equation of State for Electrolyte Solutions by Combining the Statistical Associating Fluid Theory and the Mean Spherical Approximation for the Nonprimitive Model. J. Chem. Phys. 2007, 126 (24), 244503. https://doi.org/10.1063/1.2733673.

(36) Booth, F. The Dielectric Constant of Water and the Saturation Effect. J. Chem. Phys. 1951, 19 (4), 391–394. https://doi.org/10.1063/1.1748233.
(37) Buchner, R.; Barthel, J. 9 Dielectric Relaxation in Solutions. Annu. Rep. Sect. C Phys. Chem. 2001, 97 (0), 349–382. https://doi.org/10.1039/B101629F.
(38) Booth, F. Dielectric Constant of Polar Liquids at High Field Strengths. 1955. https://doi.org/10.1063/1.1742009.
(39) Maribo-Mogensen, B.; Kontogeorgis, G. M.; Thomsen, K. Modeling of Dielectric Properties of Aqueous Salt Solutions with an Equation of State. J. Phys. Chem. B 2013, 117 (36), 10523–10533. https://doi.org/10.1021/jp403375t.
(40) Hunger, J.; Stoppa, A.; Schrödle, S.; Hefter, G.; Buchner, R. Temperature Dependence of the Dielectric Properties and Dynamics of Ionic Liquids. ChemPhysChem 2009, 10 (4), 723–733. https://doi.org/10.1002/cphc.200800483.
(41) Weiss, V. C.; Schröer, W. Macroscopic Theory for Equilibrium Properties of Ionic-Dipolar Mixtures and Application to an Ionic Model Fluid. J. Chem. Phys. 1998, 108 (18), 7747–7757. https://doi.org/10.1063/1.476210.
(42) Levy, A.; Andelman, D.; Orland, H. Dielectric Constant of Ionic Solutions: A Field-Theory Approach. Phys. Rev. Lett. 2012, 108 (22), 227801. https://doi.org/10.1103/PhysRevLett.108.227801.
(43) Helgeson, H. C.; Kirkham, D. H.; Flowers, G. C. Theoretical Prediction of the Thermodynamic Behavior of Aqueous Electrolytes by High Pressures and Temperatures; IV, Calculation of Activity Coefficients, Osmotic Coefficients, and Apparent Molal and Standard and Relative Partial Molal Properties to 600 Degrees C and 5kb. Am. J. Sci. 1981, 281 (10), 1249–1516. https://doi.org/10.2475/ajs.281.10.1249.
(44) Read Online Thermodynamic Models | pdf.wecabrio.com https://pdf.wecabrio.com/read/qjmeOgAACAAJ.pdf (accessed 2021 -06 -05).
(45) Von Hippel, A. R. Dielectrics and Waves; Wiley; Chapman & Hall: New York; London, 1954.
(46) Sen, P. N. Relation of Certain Geometrical Features to the Dielectric Anomaly of Rocks. Geophysics 1981, 46 (12), 1714–1720. https://doi.org/10.1190/1.1441178.
(47) Josh, M. Dielectric Permittivity: A Petrophysical Parameter for Shales. Petrophysics - SPWLA J. Form. Eval. Reserv. Descr. 2014, 55 (04), 319–332.
(48) Beloborodov, R.; Pervukhina, M.; Han, T.; Josh, M. Experimental Characterization of Dielectric Properties in Fluid Saturated Artificial Shales. Geofluids 2017, 2017, 1–8. https://doi.org/10.1155/2017/1019461.
(49) Saltas, V.; Vallianatos, F.; Soupios, P.; Makris, J.; Triantis, D. Application of Dielectric Spectroscopy to the Detection of Contamination in Sandstone. Int. Workshop Geoenvironment Geotech. 2005.
(50) Mukhametshina, A.; Martynova, E. Electromagnetic Heating of Heavy Oil and Bitumen: A Review of Experimental Studies and Field Applications; 2013. https://doi.org/10.1155/2013/476519.

(51) Abraham, T.; Van Neste, C.; Afacan, A.; Thundat, T. Dielectric Relaxation Based Capacitive Heating of Oil Sands. Energy Fuels 2016, 30. https://doi.org/10.1021/acs.energyfuels.5b02493.
(52) Roubinet, D.; Irving, J. Discrete-Dual-Porosity Model for Electric Current Flow in Fractured Rock. J. Geophys. Res. Solid Earth 2014, 119. https://doi.org/10.1002/2013JB010668.
(53) Al-Harahsheh, M.; Kingman, S.; Saeid, A.; Robinson, J.; Dimitrakis, G.; Alnawafleh, D. H. Dielectric Properties of Jordanian Oil Shales. Fuel Process. Technol. 2009, 90, 1259–1264. https://doi.org/10.1016/j.fuproc.2009.06.012.
(54) Donadille, J.-M. On the Petrophysical Analysis of Dielectric Anisotropy; OnePetro, 2016.
(55) Beloborodov, R.; Pervukhina, M.; Han, T.; Josh, M. Experimental Characterization of Dielectric Properties in Fluid Saturated Artificial Shales. Geofluids 2017, 2017, 1–8. https://doi.org/10.1155/2017/1019461.
(56) (PDF) The Effects of the pH-Influenced Structure on the Dielectric Properties of Kaolinite-Water Mixtures https://www.researchgate.net/publication/238773538_The_Effects_of_the_pH-Influenced_Structure_on_the_Dielectric_Properties_of_Kaolinite-Water_Mixtures (accessed 2021 -06 -05).